Automated identification of the position and orientation of the LDA measuring volume with respect to flow cross section

Automatisierte Bestimmung der Position und Ausrichtung des LDA-Messvolumens zum Strömungsquerschnitt

F. Heitmann[1], M. Juling[1], J. Steinbock[1], M. Kraume[2]

[1] Physikalisch-Technische Bundesanstalt (PTB), Abbestraße 2-12, 10587 Berlin

[2] Technische Universität Berlin, Fachgebiet Verfahrenstechnik, Straße des 17. Juni 135, 10623 Berlin

LDA, Messunsicherheit, Messvolumen, Messposition, Ortsauflösung
LDV, measurement uncertainty, measuring volume, measuring position, spatial resolution

Abstract

Positioning of the measuring volume is one of the biggest contributors to uncertainty in laser Doppler anemometry (LDA). It is even more crucial for spatially resolved LDA, where two measuring volumes have to be overlapped precisely. Therefore, a new measurement principle is presented that makes use of a glass marking on the flow confining wall. Traversing a laser beam across the glass marking causes a distinct refraction signal, which allows the localisation of the glass wall with respect to the measuring volume. With this principle, the location of the flow cross section centre is determined fully automated within 15 minutes, with a 3D combined uncertainty below 5 µm. Furthermore all three angles between measuring volume and flow cross section are measured within 4 minutes with uncertainties below 600 µrad. Using a six-axis positing system, all angles are corrected autonomously. Hence, a reproducible procedure has been developed allowing a fully automated preparation for spatially high resolved LDA measurements.

Introduction

Laser Doppler anemometry (LDA) allows high resolution measurements regarding the flow velocity inside its measuring volume. In a conventional two-beam setup the spatial resolution is limited by the length of the measuring volume.
To increase the spatial resolution, two conventional LDA probes with different wavelengths can be used to create an intersection of the two measuring volumes. Furthermore, they are configured so that one has a constant and the other one a divergent fringe spacing along the optical axis. Thereby, the particle position along their optical axis can be derived from the ratio of the signals' dominant frequencies, resulting in spatial resolution well below the measuring volumes length (Czarske et al., 2002).
This advanced principle has been used for investigation of wall-bound turbulent flows (Lowe, 2006) and free jets (Büttner et al., 2008), among others. For simple geometries, e.g. the measurement through a planar glass wall, overlapping of the two measuring volumes is independent

of the translational movement. For complex test section geometries, this is generally not the case. Instead, it might result in non-intersecting measuring volumes. For complex test section geometries, a matching of the fluids refractive index can solve these challenges (Durst et al., 1995). This is clearly not feasible for gaseous flows or investigation of flows of defined composition and temperatures.

In these cases, the LDA probes have to be positioned separately. With the aid of ray tracing to account the test section geometry, both LDA probes can be positioned independently, thereby overlapping the measuring volumes across the flow domain. For this purpose, a reference point with respect to the test section geometry must be located, e.g. the flow confining wall. Several approaches are to be found in the literature.

Durst and Müller (1988) use a hot wire anemometer, whose wall distance has been determined beforehand. The scattering of the measuring volumes light by the wire is recorded with a photomultiplier, while the measuring volume is traversed stepwise. From the Gaussian distribution of the scattered light signal along the traversing path, the centre of the measuring volume is found. However, this requires calibration with the wall material and physical access to the wall to place the hot wire anemometer. It is therefore not suitable for complex test section geometry, high temperature and pressure or aggressive fluids.

Bertrand et al. (1993) propose using a thermocouple to register its heating-up by the measuring volume light being absorbed. This also requires physical access to the test section. Additionally, the thermocouple is positioned relative to the wall using a microscope, requiring lateral optical access to the wall.

Durst et al. (1995) study near-wall flow. To locate the wall, the measuring volume is traversed to intersect with the wall. Particles adhering to the wall scatter the laser beams' light. Maximal scattering intensity is reached when the centre of the measuring volume is intersecting with the wall. To eliminate reflection on the glass/fluid-interface, the fluids refractive index has to be matched.

In this contribution a new automated calibration procedure is presented that enables the localisation of the wall without physical access to the test section or matching of refractive index. It is used to determine a glass flow pipe's centre as reference point for traversing the measuring volume in the flow cross section. In addition, the procedure allows for the measurement of all three angles between the traversing axis and the glass flow pipe. Only if these angles are known and corrected for, two measuring volumes can be traversed synchronously along the flow cross section enabling reliable and reproducible spatially resolved LDA measurements.

Glass marking and path measurement

The test section of this experimental setup consists of a borosilicate glass flow pipe with outer diameter d_{out}=88,6 mm, encased in a sight glass flow indicator. Using a rotating roundness tester equipped with a diamond cutting tool, a circumferential glass marking, 10 µm deep and 50 µm wide, has been cut into the outer wall of the glass flow pipe. A laser beam hitting the glass marking gets spread out perpendicular due to the highly altered incident angle, as is shown in figure 1 (sight glass flow indicator not depicted).

A light detector positioned downwards of the optical axis can register that process as a rise in light intensity. In this experimental setup, two opposing LDA probes are used in forward scattering mode. They include the receiving optic which is connected via optical fibre to a photomultiplier. Similar to the LDA measurement, they can be used as a detector for the opposing probe in the presented calibration procedure. The sending probe is traversed along the y-axis,
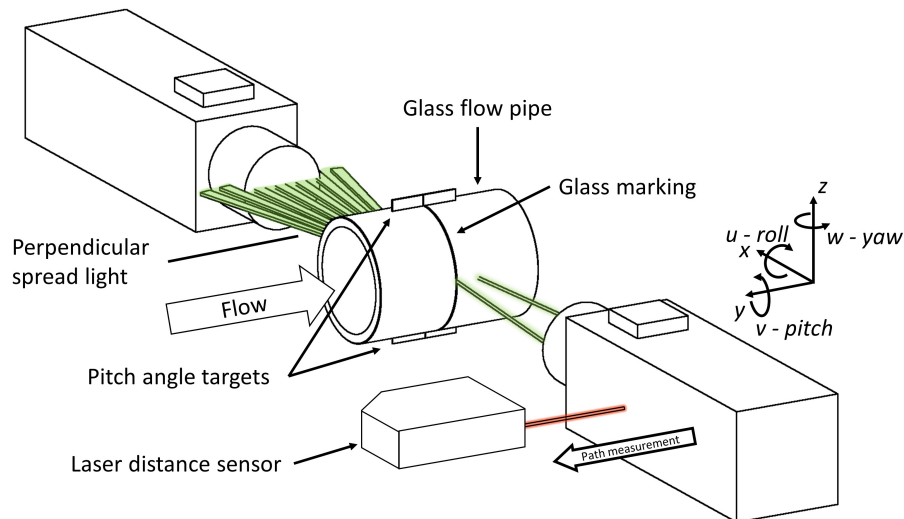
Figure 1: Beam being sent out from the right LDA probe and spread out on the glass marking of the glass flow pipe. Left LDA probe acts as the sensor for the signal. In each path measurement, the sending LDA probe is traversed along the y-axis, a laser distance sensor tracks the probes y-position.

with x and z kept constant. Due to the beams Gaussian intensity profile, such an intensity signal is registered by the receiving probe when one beam crosses the glass marking.

For a path measurement, the sending LDA probe is traversed along y for a distance of $\Delta y = 5\,\text{mm}$ at 15 mm/s, so that both beams cross the glass marking. The recorded voltage signal of the receiving photomultiplier is shown in figure 2. Parameters for two Gaussian functions are fitted
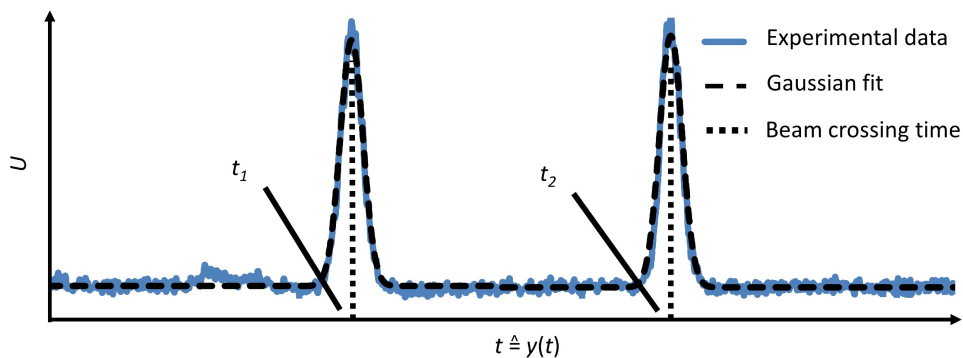
Figure 2: Voltage signal of single path measurement, recorded through a LDA probe receiving optic connected to a photomultiplier. With time resolved positioning signal of the laser distance sensor a position in y can be assigned to every t

to the data, which yield the points t_1 and t_2 that indicate the crossing of the beams. As the employed positioning system does not provide a position signal of high temporal resolution, a laser distance sensor is installed in a fixed position, monitoring the position of the sending LDA probe at 30 kHz rate, approximately along the y-axis. To negate any influence of a misaligned direction of measurement or absolute errors of the laser distance sensor, the signal is first normalised to a range of 0 to 1, giving $l_n(t)$. Together with the start- and endpoints of the traversing path y_{min} and y_{max} the y-position can be calculated as

$$y(t) = y_{min} + (y_{max} - y_{min}) \cdot l_n(t). \tag{1}$$

Therefore, a y-position can be assigned to both points in time t_1 and t_2.

Locating the glass marking

The path measurement described above is used to locate the position where the measurement volume and the glass marking coincide. For this purpose, ten path measurements are carried out at a constant height z, while in between path measurements the LDA probe is additionally traversed $\Delta x_{PM} = 4$ mm along the x-axis. Overall, the measurement takes 16 s time, covering a 5 mm by 40 mm area. This results in a total traversing path depicted in figure 3a with the beam crossing locations indicated by the Gaussian function. Signals in close proximity to each
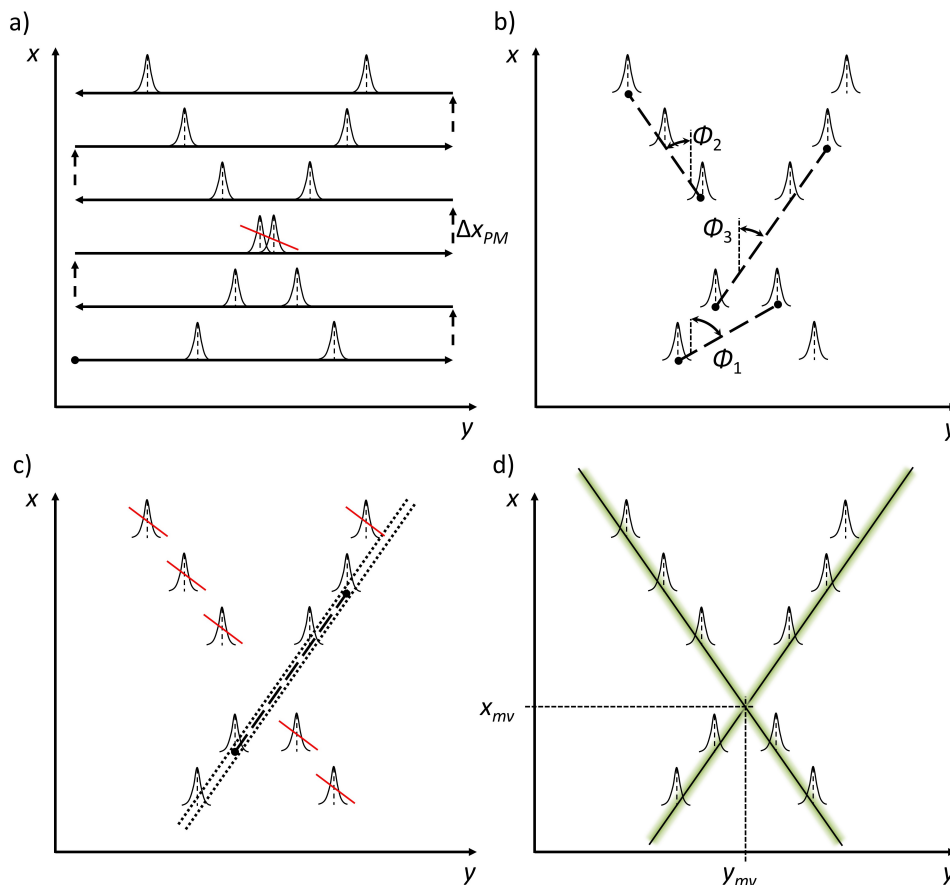
Figure 3: Modified RANSAC algorithm for beam reconstruction. a) Data from path measurements, signals in close proximity are excluded. b) Identify suitable pair of data by slope. c) Assign data to consensus. d) Intersection of beams indicates where measuring volume is located on glass marking.

other are excluded from the dataset due to ambiguity. To reconstruct the beams, a modified RANSAC (*random sample consensus*, Fischler and Bolles (1981)) algorithm is applied. As the approximate beam slope is known (beam angle from the measuring volume calibration), the slope between two random points is calculated until a pair with a slope deviating less than 1° from the beam angle is found, figure 3b. Then, in figure 3c, a subset of data points is found that deviate less than 20 µm from the line constructed before, called the consensus. The steps depicted in b and c are repeated, until a large enough consensus is found for the first beam. Accordingly, the line describing the second beam best is found. The beams intersection yields the position in x and y, where the measuring volume coincides with the glass marking for the given height z, figure 3d.
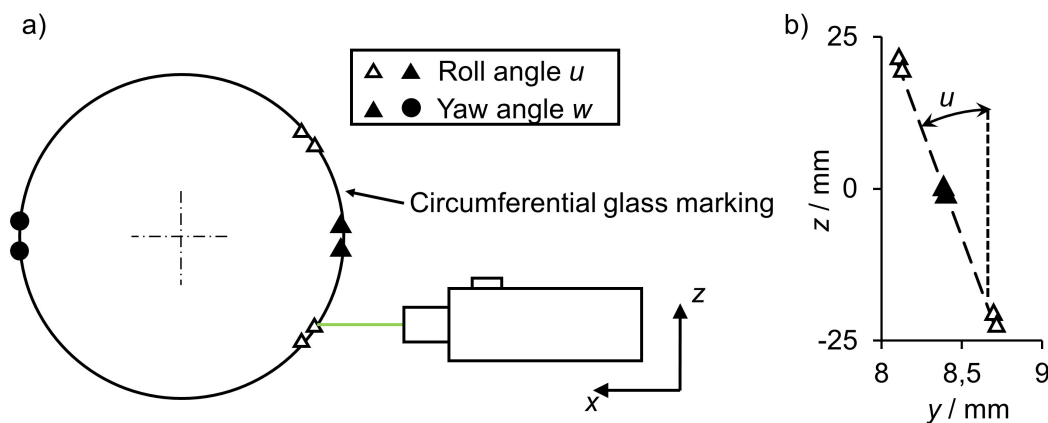
Glass flow pipe centre

In order to locate the glass flow pipe centre, the glass marking is measured in steps of $2\,\mathrm{mm}$ along the pipe height z. As the beam spreads out mostly horizontally, the receiving LDA probe is vertically traversed as well to optimise signal strength.

The glass marking on both the near and the far side of the glass flow pipe are measured in that fashion, resulting in 54 locations after 15 minutes. The results plotted in figure 4 reveal an elliptical shape, caused by refraction on the curved interfaces. Beside the measured points a fitted curve describing the x-distance between the near and far side data points for equal heights is shown (shifted in x for display). Its maximum indicates the location where the distance between the near and far side of the glass marking is greatest, i.e. the glass flow pipe's centre height z_0. Separately, the near and far side data sets can be evaluated at that height by means of a best-fit parabola, yielding $x_n(z_0)$ and $x_f(z_0)$. As the pipe geometry corresponds to a planar wall for height z_0, the centre component x_0 can easily be calculated as
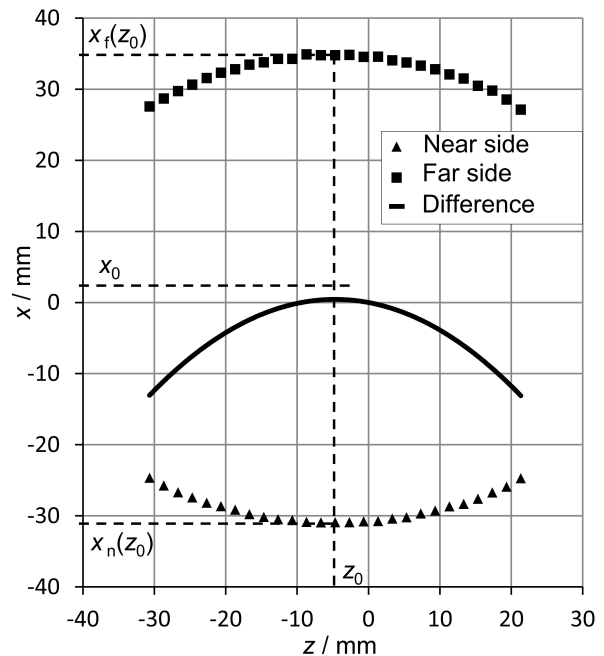
$$x_0 = \frac{x_f(z_0) - x_n(z_0)}{2}. \tag{2}$$

Figure 4: By measuring the circumferential glass marking, 54 data points are collected on the near and the far side of the glass flow pipe. The continuous line indicates difference in x between both data sets for common height z (shifted for display). Its maximum denotes pipe the centre z_0. The evaluation of best-fit parabolas for each data set yields $x_f(z_0)$ and $x_n(z_0)$. The pipe centre x_0 is found halfway between them.

Roll and yaw angle

To measure the roll angle u and the yaw angle w (compare figure 1) between the positioning system and the glass flow pipe, eight measurements of the circumferential glass marking are sufficient. Figure 5a shows the measured location on the glass marking.

Figure 5: a) Roll and yaw angle measurement locations on the circumferential glass marking. b) The roll angle u is calculated by best-fit of line in the y/z-plane.

Through the y-difference between distant points, the respective angles can be inferred. Pairs of adjacent points help suppress the influence of small irregularities in the glass marking on the results. For the roll angle u, six points across the near side glass marking are included in a linear best-fit in the y/z-plane, as is shown in figure 5b. The yaw angle w is calculated in a similar fashion using the points near z_0 and a linear fit in the x/y-plane.

Pitch angle

As the circumferential glass marking is axially symmetric, the pitch angle v can not be derived from measuring it. Instead, additional pitch angle targets were placed above and below the glass flow pipe. They consist of a 1 mm thick borosilicate glass sheet with a central vertical glass marking across the height of $h_t = 8$ mm as depicted in figure 1. It was applied with a diamond cutting tool and is approximately 80 µm wide. Like the circumferential glass marking, measurements can be carried out to locate the measuring volume on the glass marking. As it is shown in figure 6, starting at the known height z_0, the LDA probe is traversed by $(d_out + h_t)/2$ in height, reaching the approximate central height of the target. Here, the glass marking is measured just like the circumferential glass marking. The lower pitch angle target is measured accordingly. The pitch angle v can now be calculated as
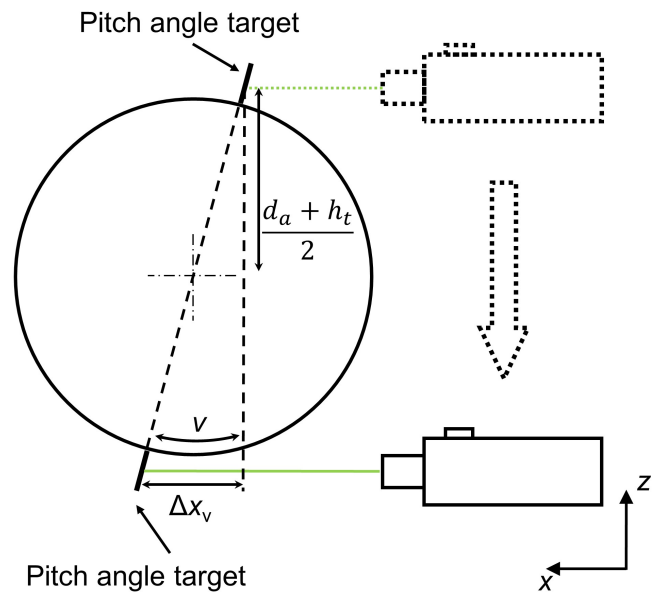
Figure 6: Glass markings on pitch angle targets above and below the glass flow pipe are measured to calculate the pitch angle v.

$$v = \tan^{-1}\left(\frac{\Delta x_v}{d_a + h_t}\right). \tag{3}$$

Measuring volume divergence due to misalignment

The procedures described above aim at providing the basis for a correction of the measured angles. In correcting the angles, the measuring volumes can be traversed together across the flow cross section without diverging from one another. The measuring volumes generated are 2000 µm in length and 150 µm in diameter. Divergence radial to the optical axis should therefore be kept well below 75 µm for each measuring volume to ensure sufficient intersection.

For the pitch angle v, a misalignment of Δv factors in to the divergence of the measuring volume in height as Δz_v, depending on the traversed length from the reference point Δx, figure 7. The corresponding equation is

$$\Delta z_v = \sin(\Delta v) \cdot \Delta x. \tag{4}$$

The other two angles contribute in a similar fashion. With an inner pipe diameter of $d_{in} = 75{,}0$ mm, the maximal traversing length from the pipe centre reference point is $\Delta x_{max} = 37{,}5$ mm. Therefore, the cutoff pitch angle for intersection is $\Delta z_{v,max} = \sin^{-1}(75$ µm $/ 37500$ µm$) = 2$ mrad.
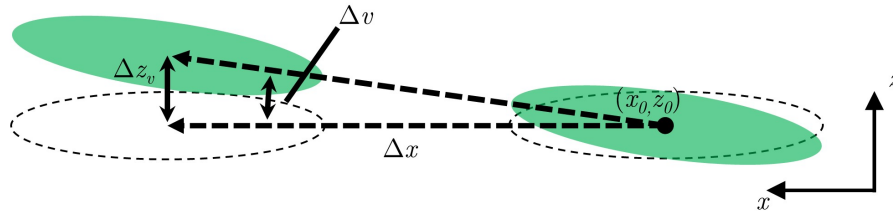
Figure 7: Divergence of the measuring volume due to pitch angle misalignment.

Positioning system

To correct the measured angles, two six-axis hexapod positioning system are used to traverse the LDA probes. On top of the three translational degrees of freedom, they also allow for rotation of the LDA probe around all three axis to align to the glass flow pipe. They achieve an absolute translational positioning of the probes with deviations below 9 μm across the entire traversing space. The rotational backlash amounts to 5 μrad, the rotational repeatability to ±0,5 μrad and the maximal absolute rotational deviation to ±48 μrad.

The angles measured following the procedures described above are corrected using the rotational degrees of freedom of the positioning systems. Subsequently, the angles are measured again, resulting in a iterative procedure of about 15 minutes.

Results and discussion

The glass flow pipe centre is measured 22 times, each measurement consists of 54 points along the glass marking, as described above. The standard deviation for each direction can be found in table 1 together with the calculated root sum squared 3D standard deviation $\sigma_{3D,0}$. Owing to the high number of points along the circumfence, low standard deviations for all axis

Table 1: Standard deviation for the glass flow pipe centre acquired through 22 measurements, individual directions and combined spatial standard deviation.

σ_{x0} / μm	σ_{y0} / μm	σ_{z0} / μm	$\sigma_{3D,0}$ / μm
2,9	3,2	1,1	4,5

are achieved. The combined spatial standard deviation amounts to 3 % of the 150 μm measuring volume diameter produced in this experimental setup, allowing for a nearly complete intersection of the measuring volumes in the glass flow pipe centre.

The procedures to determine the roll, pitch and yaw angles are carried out 20 times to obtain their respective standard deviations according to table 2.

Table 2: Standard deviation for roll angle U pitch angle v and yaw angle w from 22 measurements.

σ_u / μrad	σ_v / μrad	σ_w / μrad
73	588	33

The pitch angle stands out due to its differing measurement procedure (using pitch angle targets). A plausible reason is that the encasing glass flow indicator is obstructing a substantial

amount of light from reaching the receiving LDA probe, therefore decreasing the signal-to-noise ratio. As the pitch angle v is by far the biggest contributor to angle uncertainty by an order of magnitude, only its influence on the positioning uncertainty is presented. The influence of the positiong system's rotational uncertainty can be omitted as well, as it much smaller than than the pitch angle standard deviation. With equation 4 and σ_v the resulting standard deviation for the height at maximal traversing length Δx_{max} = 37.5 mm can be calculated, yielding σ_z = 22 μm. For the intersection of two measuring volumes, the resulting standard deviation is therefore $\sigma_{z,inter} = \sqrt{2 \cdot (22 \, \mu m)^2}$ = 31 μm. This corresponds to just above a fifth of the measuring volumes' diameter.

As a result, the measuring volumes can be traversed reliably to intersect each other over the whole travel range. With the angle measurement and correction as well as the pipe centre measurement each taking about 15 minutes, the setup can reliably be prepared for spatially resolved LDA measurement within 30 minutes.

A more in-depth discussion on the developed procedures can by found in the author's master thesis (Heitmann, 2017).

Acknowledgement

Bibliography

Bertrand, C., **Desevaux, P.**, **Prenel, J.P.**, **1993**: "Micropositioning of a measuring volume in laser Doppler anemometry", Experiments in Fluids, volume 16, pp. 70–72.

Büttner, L., **Bayer, C.**, **Voigt, A.**, **Czarske, J.**, **Müller, H.**, **Pape, N.**, **Strunck, V.**, **2008**: "Precise flow rate measurements of natural gas under high pressure with a laser Doppler velocity profile sensor", Experiments in Fluids, volume 45, no. 6, pp. 1103–1115.

Czarske, J., **Büttner, L.**, **Razik, T.**, **Müller, H.**, **2002**: "Boundary layer velocity measurements by a laser Doppler profile sensor with micrometre spatial resolution", Measurement Science and Technology.

Durst, F., **Jovanovic, J.**, **Sender, J.**, **1995**: "LDA measurements in the near-wall region of a turbulent pipe flow", Journal of Fluid Mechanics.

Durst, F., **Müller, R.**, **1988**: "Determination of the measuring position in laser-Doppler anemometry", Experiments in Fluids, volume 6, pp. 105–110.

Fischler, M.A., **Bolles, R.C.**, **1981**: "Random sample consensus: a paradigm for model fitting with applications to image analysis and automated cartography", Communications of the ACM, volume 24, no. 6.

Heitmann, F., **2017**: "Höchstpräzise Positionierung für die Laser-Doppler-Anemometrie mittels Hexapoden", Master's thesis, Technische Universität Berlin.

Lowe, K.T., **2006**: "Design and application of a novel Laser-Doppler Velocimeter for turbulence structural measurements in turbulent boundary layers", Ph.D. thesis, Virginia Polytechnic Institute and State University.